



THE QUADRATIC PROPORTIONALITY FACTORS OF THE ARSENIC AND ANTIMONY DIFFUSION COEFFICIENTS IN GERMANIUM WITH THE FREE ELECTRON CONCENTRATION

M.Y. Rachedi^{a,d}, A. Souigat^{b,d}, Y. Benkrima^b, Z. Korichi^b, D. Slimani^b, D. Bechki^{c,d}

^aFaculty of Modern Technologies of Informations & Communication, University of Ouargla, 30000 Ouargla, Algeria

^bEcole Normale Supérieure de Ouargla, 30000 Ouargla, Algeria

^cFaculty of Mathematics & Matter Sciences, University of Ouargla, 30000 Ouargla, Algeria

^dLENREZA Laboratory, University of Ouargla, 30000 Ouargla, Algeria

Correspondence: E-Mail: rachedi.yacine@univ-ouargla.dz

Received: 02/06/2023; Accepted: 06/09/2023; Published: 16/09/2023

Abstract

Due to its unique physical characteristics like high intrinsic carrier mobility, small band gap, and possible monolithic integration with silicon (Si) based devices, germanium (Ge) has recently emerged as a promising candidate in order to enhance the supplementary metal oxide semiconductors (CMOS) devices. Obtaining effective electronic devices based on germanium requires knowledge of the diffusion characteristics of the dopants in this semiconductor. At most, a diffusion coefficient proportional to the square of the free electron concentration (n) has been used thus far to describe the diffusion of arsenic (As) and antimony (Sb) in germanium. By simulating experimental As and Sb diffusion profiles in Ge, this paper establishes the temperature dependence of the quadratic proportionality factors of the diffusion coefficients of arsenic and antimony in germanium with free electron concentration. By accounting for the quadratic proportionality between the diffusion coefficient and the free electron concentration, an accurate simulation is achieved.

Keywords: arsenic, antimony, proportionality factor, germanium.

DOI Number: 10.48047/nq.2023.21.7.nq23009

NeuroQuantology2023;21(7):81-87

1. INTRODUCTION

Over the past decade, traditional silicon complementary metal oxide semi-conductors (CMOS) devices have been reaching their fundamental limits in terms of dimensional scaling, prompting numerous studies to investigate the introduction of new structures and materials to enable this technological advance and maintain the historic evolution made in information processing and transmission [1–5]. Germanium is an excellent choice to further

develop (CMOS) devices because of its unique physical qualities, such as its strong intrinsic carrier mobility, narrow band gap, and the possibility of monolithic integration with Si based devices [5-13]. Due to its narrower direct band gap (0.8 eV), germanium is well-suited for use in photo detectors operating at wavelengths between 1.3 and 1.55 μm [14,15], making it an attractive material for a wide variety of optical applications. It is also compatible with thermal stability requirements when integrating the metal



gate electrodes and the new high-k dielectrics into the developed transistors [16-18], and the smaller direct band gap and lower melting point of germanium aid in the fabrication of electronic devices with lower operating voltage and lower thermal cost, which is in line with the international technology roadmap for semiconductors [6,14].

Understanding the characteristics of the diffusion of dopants in germanium is crucial for producing high-performance electronic devices based on this semiconductor. Diffusion of dopants in semiconductors is linked to point defects, through which mass transport occurs. The vacancies in Ge mediate the bulk transfer of the n-type dopants [19-22]. So far, the best model for the diffusion of n-type dopants in germanium has been a coefficient of diffusion proportional to the square of the free electron concentration (n) [21-25]. The substitutional dopant donor and the singly negatively charged mobile donor-vacancy

$$D_A = \alpha_A n^2 \tag{1}$$

α_A is the quadratic proportionality factor of diffusion coefficient with the free electron concentration. A indicates the diffuse dopant, $A \in \{As, Sb\}$. From the mass action law and under the assumption of charge neutrality, the concentration of free electron carriers (n) can be calculated as follows:

$$n = \frac{1}{2} \left(C + \sqrt{C^2 + 4n_i^2} \right) \tag{2}$$

Where C and n_i are the local dopant concentration and the intrinsic carrier concentration, respectively. n_i is given by the following relationship from reference [22]:

$$n_i = \left(7.3_{-3.1}^{+5.4} \right) \times 10^{20} \exp \left(- \frac{(0.44 \pm 0.05) (eV)}{k_B T} \right) \text{ cm}^{-3} \tag{3}$$

By include the resulting term due to an internal electric field, we may characterize the overall flux J of diffuse dopant in germanium as follows.

$$J = -D_A \frac{\partial C}{\partial x} - D_A \frac{C}{n} \frac{\partial n}{\partial x} \tag{4}$$

The preservation of the diffused mass quantity is represented by the equation of continuity:

$$\frac{\partial C}{\partial t} = - \frac{\partial J}{\partial x} \tag{5}$$

From the equations (1),(2),(4)and (5) the dopant diffusion in Ge can be expressed by the following equation:

$$\frac{\partial C}{\partial t} = \frac{\partial}{\partial x} \left(D^{eff} \frac{\partial C}{\partial x} \right) \tag{6}$$

Where, x and t are the spatial coordinate and the time, respectively.

D^{eff} is the effective diffusion coefficient, is expressed as follows:

pair account for the quadratic proportionality [22,24-26].

The primary objective of this work is to simulate the experimental diffusion profiles of arsenic and antimony in Ge from reference [22] in order to gain an understanding of the quadratic proportionality factors of these element's diffusion coefficients in germanium with the free electron concentration.

2. MODEL USED

Although it appears to be well-established that Arsenic and Antimony diffusion in Ge is vacancy-mediated [21-26], we assumed that diffusion occurs through doubly negatively charged vacancies in the form of dopant-defect pairs or simple exchange, which results in a diffusion coefficient proportional to the square of the free electron concentration (n) and can be modelled using the following simple expression:

$$D^{eff} = h\alpha n^2 \tag{7}$$

h is an improvement factor arising due to an internal electric field:

$$h = 1 + \frac{C}{2n_i} \left(\left(\frac{C}{2n_i} \right)^2 + 1 \right)^{-1/2} \tag{8}$$

3. NUMERICAL SIMULATION

3.1 Numerical Treatment of Diffusion Equation

Equation (6) is solved exactly using the implicit finite difference scheme and the finite difference method. The precision of this technique is of the order $O(\Delta t, \Delta x^2)$. The concentration at time $j\Delta t$ is proportional to the concentration at time $(j-1)\Delta t$, leading to the following relationship:

$$C_i^{j-1} = -\delta_i^j C_{i-1}^j + (1 + \delta_i^j + \delta_{i+1}^j) C_i^j - \delta_{i+1}^j C_{i+1}^j \tag{9}$$

Where $\delta_i^j = \delta_0 (D^{eff})_i^j$ and $\delta_0 = \frac{\Delta t}{\Delta x^2}$

By using the no-flux boundary conditions, we obtain:

$$C_0^j = C_1^j \tag{10}$$

$$C_k^j = C_{k+1}^j \tag{11}$$

From (13-15) we get the tridiagonal matrix systems that bind the concentration at time $j\Delta t$ and the concentration at time $(j-1)\Delta t$ in the form $Bc=a$, where

$$a = \begin{pmatrix} C_1^{j-1} \\ C_2^{j-1} \\ C_3^{j-1} \\ \dots \\ C_i^{j-1} \\ \dots \\ C_k^{j-1} \end{pmatrix} \quad c = \begin{pmatrix} C_1^j \\ C_2^j \\ C_3^j \\ \dots \\ C_i^j \\ \dots \\ C_k^j \end{pmatrix} \quad \text{and}$$

$$B = \begin{pmatrix} 1 + \delta_2^j & -\delta_2^j & 0 & \dots & \dots & \dots & \dots & \dots & \dots \\ -\delta_2^j & 1 + \delta_2^j + \delta_3^j & -\delta_3^j & 0 & \dots & \dots & \dots & \dots & \dots \\ 0 & -\delta_3^j & 1 + \delta_3^j + \delta_4^j & -\delta_4^j & 0 & \dots & \dots & \dots & \dots \\ \dots & \dots & \dots & 0 & -\delta_i^j & 1 + \delta_i^j + \delta_{i+1}^j & -\delta_{i+1}^j & 0 & \dots \\ \dots & \dots & \dots & \dots & \dots & \dots & \dots & 0 & -\delta_k^j & 1 + \delta_k^j \end{pmatrix}$$

3.2 Key components of our diffusion simulation programme

For solving the obtained tridiagonal matrix systems, we developed a program in the FORTRAN programming language to mimic the experimental profiles of arsenic and antimony diffusion in germanium at the temperatures and times listed in table 1 and table 2.

The dopant concentration C_0 at surface of the germanium sample, is considered in variable throughout the diffusion $C_{j-1} = C_0$ ($j=1, 2, \dots, n_t$), the

initial conditions is $C_i = 0$ ($i=2, 3, \dots, k$), where k and n_t are the total number of space step and total number of time step, respectively.

Because the effective diffusion coefficient changes as time progresses, it must be recalculated at each time step. This coincident between theoretical and actual profiles led us to select values for α_A and intrinsic carrier density at diffusion temperature T . The domain of possible n_i -values is given by the relational domain shown by the equation (3).



Table 1. Different coefficients used in the simulations of As diffusion profiles

C_0 (cm ⁻³)	t(s)	T (°c)	n_i (cm ⁻³)	α_{As} (cm ⁸ s ⁻¹)
1.3×10^{17}	864000	640	3.00×10^{18}	3.56×10^{-51}
1.9×10^{17}	259200	680	3.40×10^{18}	1.13×10^{-50}
2.7×10^{18}	345600	730	6.20×10^{18}	3.76×10^{-50}
1.3×10^{18}	10800	920	9.10×10^{18}	1.27×10^{-48}
8.8×10^{17}	18000	868	7.00×10^{18}	6.43×10^{-49}

Table 2. Different coefficients used in the simulations of Sb diffusion profiles

C_0 (cm ⁻³)	t(s)	T (°c)	n_i (cm ⁻³)	α_{Sb} (cm ⁸ s ⁻¹)
2.4×10^{18}	1555200	600	2.20×10^{18}	6.87×10^{-51}
5.1×10^{18}	1814400	650	3.10×10^{18}	2.68×10^{-50}
5×10^{18}	259200	700	4.30×10^{18}	5.17×10^{-50}
7.5×10^{18}	259200	750	5.00×10^{18}	1.56×10^{-49}
9.8×10^{18}	72000	825	7.65×10^{18}	5.67×10^{-49}
6.3×10^{18}	14400	900	7.00×10^{18}	3.49×10^{-48}

4. RESULTS AND DISCUSSION

We compare the experimental profiles of arsenic and antimony diffusion in Ge at the relevant temperatures and periods with the simulated patterns (solid lines) shown in Fig. 1 and Fig.2.

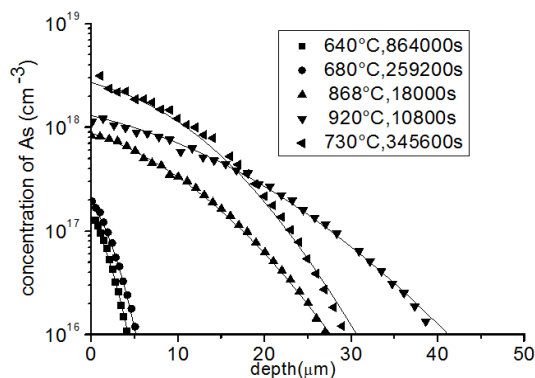


Figure 1. Comparison between the simulation (represented by solid lines) and the experimental (Reference [22]) of arsenic diffusion in germanium

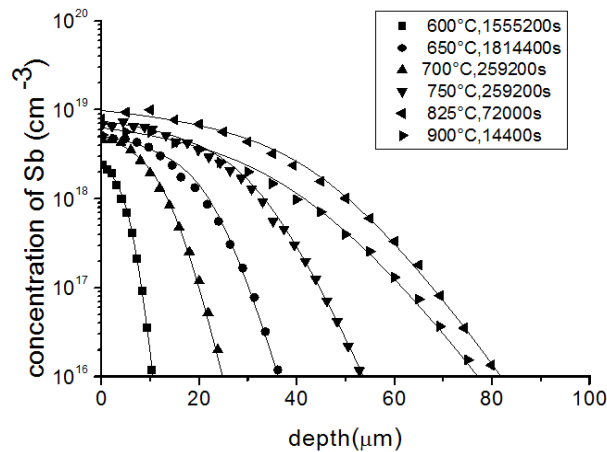


Figure 2. Comparison between the simulation (represented by solid lines) and the experimental (Reference [22]) of antimony diffusion in germanium

Using the values of the quadratic proportionality factors that we have chosen, we find that the diffusion coefficients of arsenic and antimony are proportional to the square of the free electron concentration (Fig. 1 and Fig. 2).

In Figs. 3 and 4, we present simulation results showing how the quadratic proportionality factors of the Arsenic and antimony diffusion coefficient in germanium with the free electron concentration vary as a function of the inverse of the temperature.

85

The following formulas accurately approximate the temperature dependence of the quadratic proportionality factors of As and Sb:

$$\alpha_{As} = 0.91 \times 10^{-40} \exp\left(-\frac{1.86 \text{ (eV)}}{k_B T}\right) \text{ cm}^8 \text{ s}^{-1} \tag{12}$$

$$\alpha_{Sb} = 4.6 \times 10^{-41} \exp\left(-\frac{1.7 \text{ (eV)}}{k_B T}\right) \text{ cm}^8 \text{ s}^{-1} \tag{13}$$

Where T and k_B are the temperature in kelvins and the constant of Boltzmann, respectively.

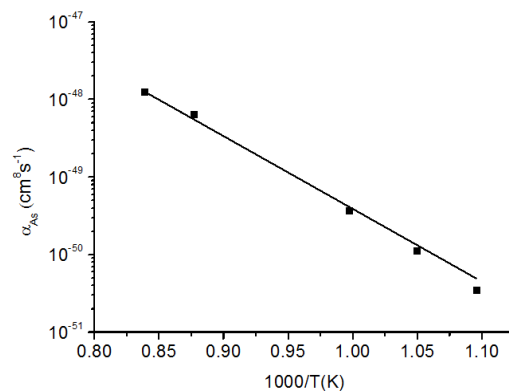


Figure 3. Variation of α_{As} with the inverse of the temperature

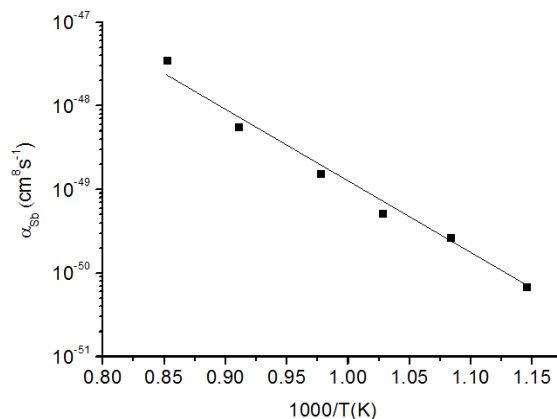


Figure 4. Variation of α_{sb} with the inverse of the temperature

5. CONCLUSION

Based on modulating the diffusion by the vacancy mechanism and accounting for the quadratic proportionality between the diffusion coefficient and the free electron concentration, this work successfully simulates experimental diffusion profiles of arsenic and antimony in germanium. Using this model, we were able to calculate the quadratic proportionality factor between As and Sb temperatures. Best reproducing the quadratic proportionality factors for As and Sb are equations (12) and (13), respectively.

REFERENCES

1. Z. Ma, D. G. Seiler, "Metrology and Diagnostic Techniques for Nanoelectronics". Jenny Stanford Publishing, (2017).
2. N. Collaert, "High Mobility Materials for CMOS Applications", Elsevier Ltd, (2018).
3. E. Summary, "The International Roadmap for Devices and Systems», Executive Summary (2017).
4. E. Simoen, C. Claeys, "Germanium Based Technologies: From Materials to Devices". Elsevier: Amsterdam (2007).
5. W. Xiong, J W. Wang, W J. Fan, et al, "The theoretical direct-band-gap optical gain of Germanium nanowires", Sci Rep. **10**, 32 (2020). <https://doi.org/10.1038/s41598-019-56765-5>
6. Mart Graef, Bert Huizing, Reinhard Mahnkopf, "The International Technology Roadmap for Semi-conductors 2.0", Executive Report, (2015).
7. U. Otuonye, H. W. Kim, and W. D. Lua, "Ge nanowire photodetector with high photoconductive gain epitaxially integrated on Si substrate", Appl. Phys. Lett. **110**, 173104 (2017). <https://doi.org/10.1063/1.4982648>.
8. S. Lee, "Advanced Material and Device Applications with Germanium". Intech Open, (2018).
9. E. N. Sgourou, Y. Panayiotatos, R. V. Vovk, et al, " Diffusion and Dopant Activation in Germanium: Insights from Recent Experimental and Theoretical Results", Appl Sci. **9**, 2454 (2019). <https://doi.org/10.3390/app9122454>
10. Z. Liu, W. Juanjuan, L. Chuanbo, et al., "Research progress of Ge on insulator grown by rapid melting growth ", J Semicond, **39**, 061005 (2018). <https://doi.org/10.1088/1674-4926/39/6/061005>
11. B. W. Cheng, C. Li, Z. Liu, et al, "Research progress of Si-based germanium materials and devices", J Semicond, **37**,081001 (2016). <https://doi.org/10.1088/1674-4926/37/8/081001>
12. P.Nguyen, M.Clavel, P goley, et al," Heteroepitaxial Ge MOS Devices on Si Using Composite AIAs/GaAs Buffer" Journal of the Electron Devices Society. **3**,341(2015). <https://doi.org/10.1109/JEDS.2015.2425959>
13. M. K. Hudait, M. Clavel, P. Goley, et al,

- “Heterogeneous Integration of Epitaxial Ge on Si using AlAs/GaAs Buffer Architecture: Suitability for Low-power Fin Field-Effect Transistors”, *Sci Rep.***4**, 6964 (2014).
<https://doi.org/10.1038/srep06964>
14. K. C. Saraswat, D. Kim, T Krishnamohan, et al, “ Germanium for High Performance MOSFETs and Optical Interconnects”, *ECS Transactions.* **16**, 3 (2008).
 15. C. Monmeyrana, I. F. Croweb, R. M. Gwilliamc, et al, “ Strategies for increased donor electrical activity in germanium (opto-) electronic materials: a review”, *International Materials Reviews.***62**,334 (2017).
<https://doi.org/10.1080/09506608.2016.1261223>
 16. P. S. Goley, M. Hudait, “ Germanium Based Field-Effect Transistors: Challenges and Opportunities” *Materials.***7**, 2301 (2014).
<https://doi.org/10.3390/ma7032301>.
 17. Y. Kamata, “ High-k/Ge MOSFETs for future nanoelectronics”, *Mater Today.***11**, 30 (2008).
[https://doi.org/10.1016/S1369-7021\(07\)70350-4](https://doi.org/10.1016/S1369-7021(07)70350-4)
 18. S. Abermann, C. Henkel, O. Bethge, et al, Stabilization of a very high-k crystalline ZrO₂ phase by post deposition annealing of atomic layer deposited ZrO₂/La₂O₃ dielectrics on germanium”, *Appl Surf Sci.***256**,5031 (2010).
 19. T. Kalliovaara, J. Slotte, I. Makkonen, et al, *Applied Physics Letters.***109**,182107(2016).
 20. C. Thomidis, M. Barozzi, M Bersani, et al, “ Strong Diffusion Suppression of Low Energy–Implanted Phosphorous in Germanium by N₂ Co-Implantation”, *ECS Solid State Letters.***4**, 47 (2015).
<https://doi.org/10.1149/2.0061506ssl>
 21. E. Simoen, J. Vanhellefont, “ On the diffusion and activation of ion-implanted n-type dopants in germanium” *J Appl Phys.* **106**, 103516 (2009).
<https://doi.org/10.1063/1.3261838>.
 22. S. Brotzmann, H Bracht, “ Intrinsic and extrinsic diffusion of phosphorus, arsenic, and antimony in germanium” *J Appl Phys.***103**, 033508 (2008).
<https://doi.org/10.1063/1.2837103>.
 23. S. Koffel, R. J. Kaiser, A. J. Bauer, et al, “ Experiments and simulation of the diffusion and activation of the n-type dopants P, As, and Sb implanted into germanium “, *Microelectronic Engineering.***88**, 458 (2011).
[DOI: 10.1016/j.mee.2010.09.023](https://doi.org/10.1016/j.mee.2010.09.023)
 24. A. Chronos, H. Bracht, “ Diffusion of n-type dopants in germanium” *Appl. Phys. Rev.* **1**, 011301 (2014).
<https://doi.org/10.1063/1.4929762>
 25. J. K. Prübing , G. Hamdana, D. Bougeard et al, “Quantitative scanning spreading resistance microscopy on n-type dopant diffusion profiles in germanium and the origin of dopant deactivation “, *J Appl Phys.***125**, 085105 (2019). ;
<https://doi.org/10.1063/1.5066617>
 26. P. Tsouroutas, D. Tsoukalas, H. Bracht, “ Experiments and simulation on diffusion and activation of codoped with arsenic and phosphorous germanium”, *J Appl Phys.* **108**, 024903 (2010).